

## Supporting Information

### **Controllable Fabrication of Redox-active Conjugated Microporous Polymer on Reduced Graphene Oxide for High Performance Faradaic Energy Storage**

Abdul Muqsit Khattak,<sup>‡ab</sup> Haksong Sin,<sup>‡a</sup> Zahid Ali Ghazi,<sup>a</sup> Xiao He,<sup>a</sup> Bin Liang,<sup>a</sup> Niaz Ali Khan,<sup>a</sup> Hamideh Rezvani Alanagh,<sup>a</sup> Azhar Iqbal,<sup>a</sup> Lianshan Li<sup>\*a</sup> and Zhiyong Tang<sup>\*a</sup>

#### **Materials**

All the chemicals used for synthesis were of analytical grade and were used without further purification. Graphite (CP grade,  $\leq 300$  mesh) and activated carbon (CP grade) were purchased from Sinopharm Chemical Reagent. *N,N*-dimethylformamide, acetone, chloroform and absolute ethanol ( $\geq 99.7\%$ ) were bought from Beijing Chemical Works. 1, 3, 5-triethynylbenzene ( $\geq 97\%$ ), *p*-diaminobenzene ( $\geq 99.7\%$ ), 1, 1'-dibromoferrocene, [Pd(PPh<sub>3</sub>)<sub>4</sub>], cetyltrimethyl ammonium bromide (CTAB), CuI and triethylamine (Et<sub>3</sub>N) were achieved from Sigma Aldrich.

#### **Synthetic methodologies**

##### **Synthesis of conjugated microporous polymers without (CMPs) and with (Fc-CMPs) ferrocene moieties**

Conjugated microporous polymers (CMPs) without and with ferrocene moieties (Fc-CMPs) were synthesized via Sonogashira cross-coupling polycondensation of 1, 3, 5-triethynylbenzene (TEB, 0.33 mmol) and dibromobenzene (DBB, 1mmol) or 1, 1'-dibromoferrocene (DBF, 1mmol) in the presence of [Pd(PPh<sub>3</sub>)<sub>4</sub>] (15 mg), CuI (7 mg) and Et<sub>3</sub>N (5 mL) in a 50 mL two-neck flask. The polymerization reactions of TEB and DBF were carried out in a mixture of *N,N*-dimethylformamide (DMF) and triethylamine (Et<sub>3</sub>N) by heating the reaction mixture to 90°C, with continuous stirring for 48 h under N<sub>2</sub> atmosphere. Then, the insoluble precipitated polymer networks were collected by filtration and washed repetitively with acetone, THF, chloroform and water followed by Soxhlet extraction with acetone for 48 h. The product was dried in vacuum for 12 h at 100°C.

##### **Synthesis of 2D composites of reduced graphene oxide and conjugated microporous polymers with (Fc-CMPs/rGO) or without (CMPs/rGO) ferrocene**

Synthesis of 2D composites of reduced graphene oxide (rGO) and conjugated microporous polymer with ferrocene moieties (Fc-CMPs) was performed by using Sonogashira-Hagihara reaction. First, graphene oxide (GO) was synthesized by a modified

Hummer's method according to previous literature.<sup>1</sup> Then GO was reduced with hydrazine hydrate<sup>2</sup> and functionalized by treatment with a *p*-bromobenzene diazonium salt under aqueous conditions.<sup>3</sup> The obtained bromo-functionalized rGO (rGO-Br) was dispersed in DMF. Then 1, 3, 5-triethynylbenzene (0.33 mmol), 1, 1-dibromoferrocene (1 mmol), [Pd(PPh<sub>3</sub>)<sub>4</sub>] (15 mg), CuI (7 mg) and Et<sub>3</sub>N (5 mL) were added to the rGO-Br dispersion. The reaction mixture was heated to 85°C and stirred for 48 h under N<sub>2</sub> atmosphere. Then, the insoluble precipitated polymer networks were filtered and washed four times with acetone, THF, chloroform, water and methanol to remove any unreacted monomers or catalyst residues. Further purification of the polymer networks was carried out by Soxhlet extraction with acetone for 48 h. The product was dried in vacuum for 12 h at 100°C. For comparison, 2D composites of rGO and CMPs without ferrocene (CMPs/rGO) were also prepared using 1, 4-dibromobenzene (DBB) monomer under the same Sonogashira-Hagihara reaction.

### **Structural and morphological characterization**

As-synthesized products were thoroughly characterized by different techniques. Surface morphology, composition and elemental mapping were performed on scanning electron microscopy (SEM) (model: Hitachi S4800) and Transmission electron microscope (TEM) (model: FEI Tecnai G2 F20). Fourier transform infrared (FTIR) spectra were collected (model: Spectrum One) in the spectral range of 400-4000 cm<sup>-1</sup> using the KBr disk method. To evaluate the valance band position of the products, XPS spectra were performed on an ESCALAB 250 Xi XPS system of Thermo Scientific, where the analysis chamber was 1.5×10<sup>-9</sup> mbar and the X-ray spot was set to 500 μm. The BET (Brunauer-Emmett-Teller) surface area, pore volume and pore size of the products were measured using a Micromeritics ASAP 2420 system instrument.

### **Electrochemical characterization**

Electrochemical studies were carried out in conventional three-electrode and two-electrode symmetric supercapacitor setup, respectively, under room temperature with 1 M H<sub>2</sub>SO<sub>4</sub> aqueous solution as the electrolyte. Briefly, in three-electrode system, CMPs, CMPs/rGO, Fc-CMPs or Fc-CMPs/rGO on graphite plate was employed as the working electrode, platinum (Pt) foil and Ag/AgCl electrodes were used as the counter and reference electrodes, respectively. The working electrodes for all samples were prepared by mixing 80 wt% active materials, 8 wt% polyvinylidene difluoride (PVDF) binder and 12 wt% carbon black in an agate mortar. Then an appropriate amount of ethanol was added to this mixture to make slurry, which was subsequently coated on graphite plates and dried in an oven at 100°C for 10 h. The mass loading of the sample was 0.85 mg/cm<sup>2</sup>.

While in a traditional two-electrode system, for Fc-CMPs/rGO symmetric system, 80% active material slurry was pasted on graphite plates (1.2 cm × 1.2 cm × 0.3 cm) and then two plates with equal amount of active materials were immersed in a beaker containing 1 M H<sub>2</sub>SO<sub>4</sub>. The distance between the two plates was around 3 mm.

The electrochemical performance of the assembled devices was studied on a CHI660D electrochemical workstation using cyclic voltammetry (CV) at various scan rates, galvanostatic charge-discharge (GCD) curves at different current density from 0.5 A/g to 10 A/g for both three-electrode and two-electrode systems at room temperature. The voltage window employed in three-electrode system was 0.8 V, while 1.0 V potential window was used in two-electrode system. The specific capacitance ( $C_s$ ) was calculated from the slop of discharge curve using the following formula:

In the three-electrode measurement, the specific capacitance was calculated from charge-discharge profiles using the following equation:

$$C_s = I \times \Delta t / m \times \Delta V$$

As for two-electrode symmetric system, the following equation was used to calculate the specific capacitance:

$$C_s = 2 \times I \times \Delta t / m \times \Delta V$$

The volumetric capacitance of the devices was calculated using the following formula:

$$C_v = I / V \times \Delta t / \Delta V$$

The gravimetric energy density (E) and power densities (P) of the device were calculated using the following formulas:

$$E = 1/8 C_s (\Delta V)^2$$

$$P = E / \Delta t$$

where  $C_s$  was the specific capacitance of supercapacitor,  $C_v$  was the volumetric capacitance, I corresponded to the discharge current,  $\Delta V$  was the potential window,  $\Delta t$  was the discharge time, V was the volume of electrode, and m referred to the mass of active materials on one electrode.

The theoretical pseudocapacitance (507.1 F g<sup>-1</sup>) of Fc-CMPs based on the molecular weight (238 g mol<sup>-1</sup>) of the repeating unit was calculated by the previously reported method:

Capacitance:  $n \times F / M_w \times 3.6 = 1 \times 96485 / 238 \times 3.6 = 112.7 \text{ mA h g}^{-1}$ , where n is the electron transfer number; F is the Faraday constant (C mol<sup>-1</sup>);  $M_w$  is the molar weight (g mol<sup>-1</sup>).

Converting to F g<sup>-1</sup>:  $= 112.7 \text{ mA h g}^{-1} \times 3600 \text{ h}^{-1} \times A / 1000 \text{ mA} = 405.7 \text{ A s g}^{-1}$

Considering the 0.8 V window studied:  $405.7 \text{ A s g}^{-1} \times 1 / 0.8 \text{ V} = 507.1 \text{ F g}^{-1}$

## Additional Figures

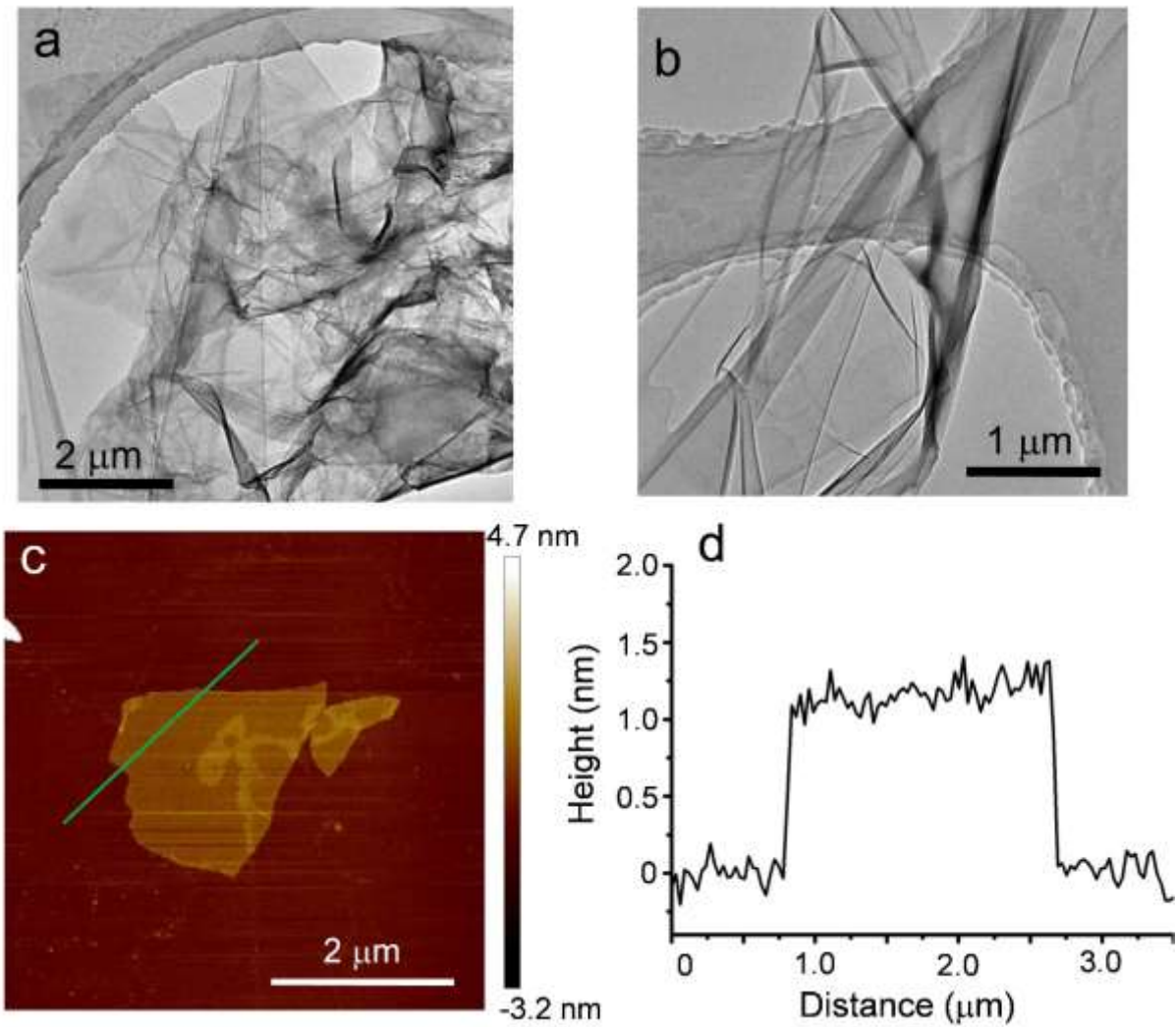


**Figure S1.** TEM images (a, b), and AFM image (c) and corresponding height profile (d) of GO monolayer nanosheets.

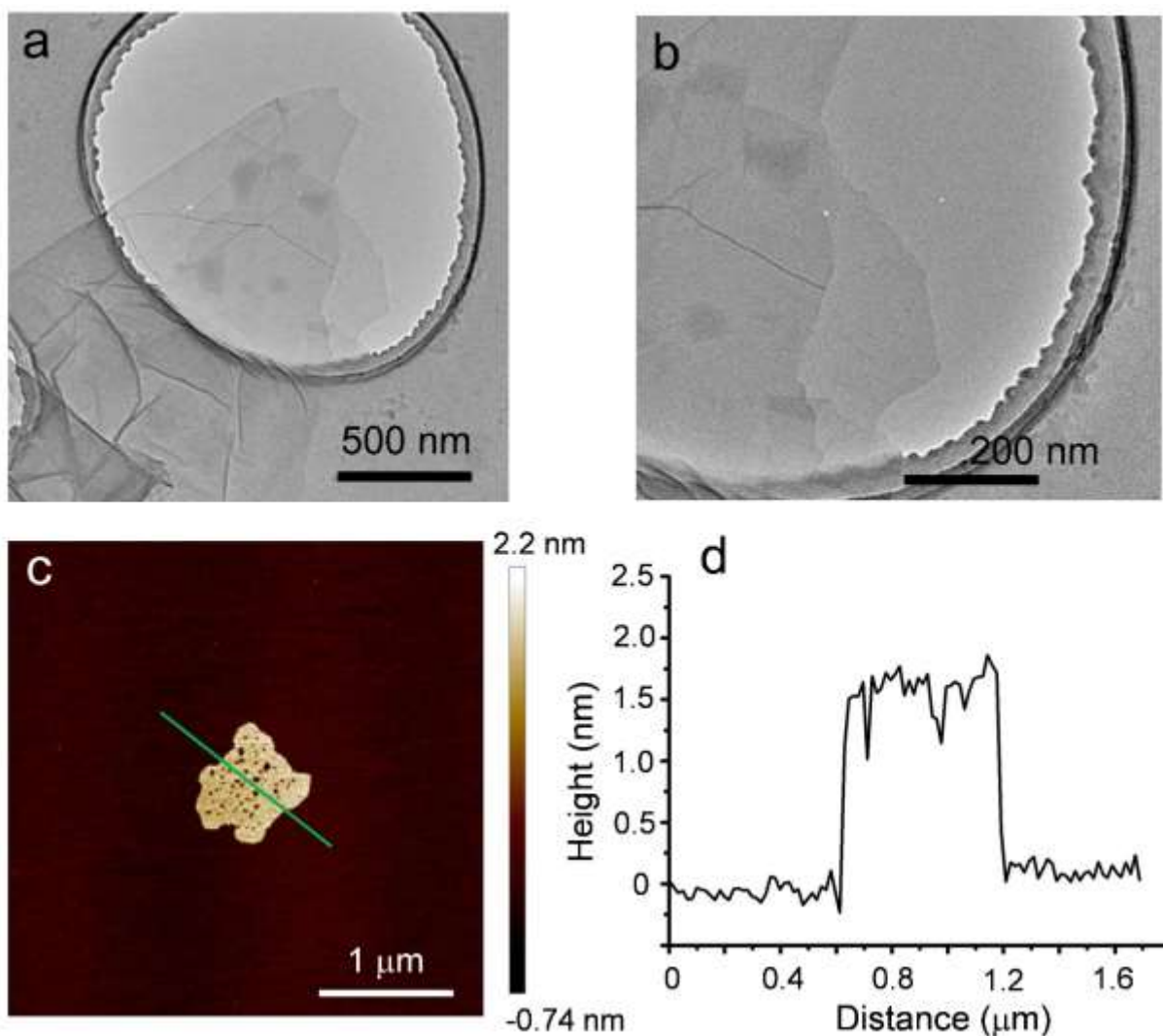


**Figure S2.** TEM images (a, b), and AFM image (c) and corresponding height profile (d) of bromobenzene modified rGO nanosheets.

Considering the fact that the monolayer bromobenzene molecules might be tilted on the surface of rGO, the thickness of bromobenzene modified rGO is thinner than the theoretical thickness of 2.12 nm if we assume that rGO is modified by monolayer of bromobenzene on both sides. The holes on the surface might be caused by chemical reactions happened during modification.

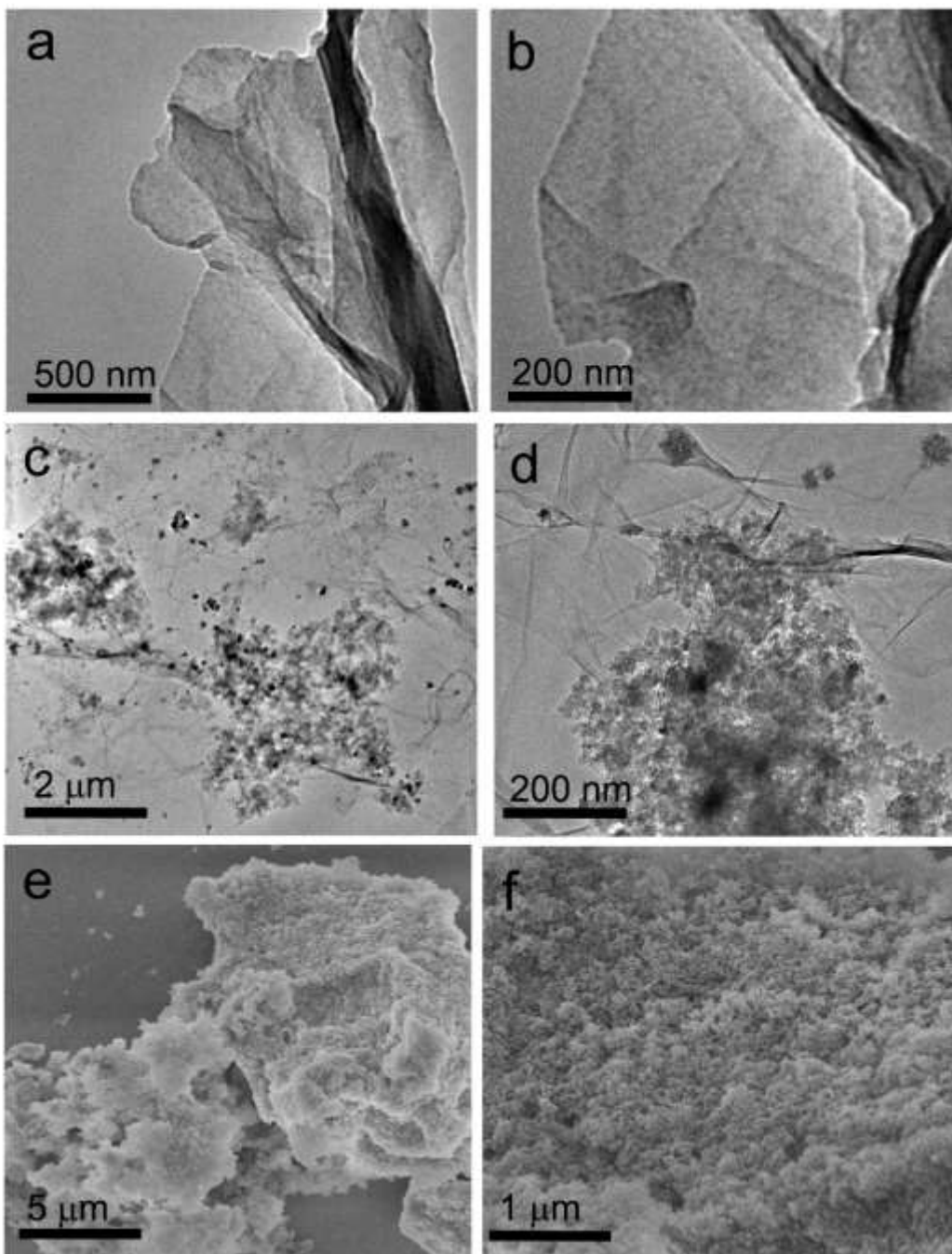


**Figure S3.** TEM images of 2D Fc-CMPs/rGO composites synthesized with rGO-Br (a, b) and rGO (c, d), and SEM images of pure Fc-CMPs (e, f).

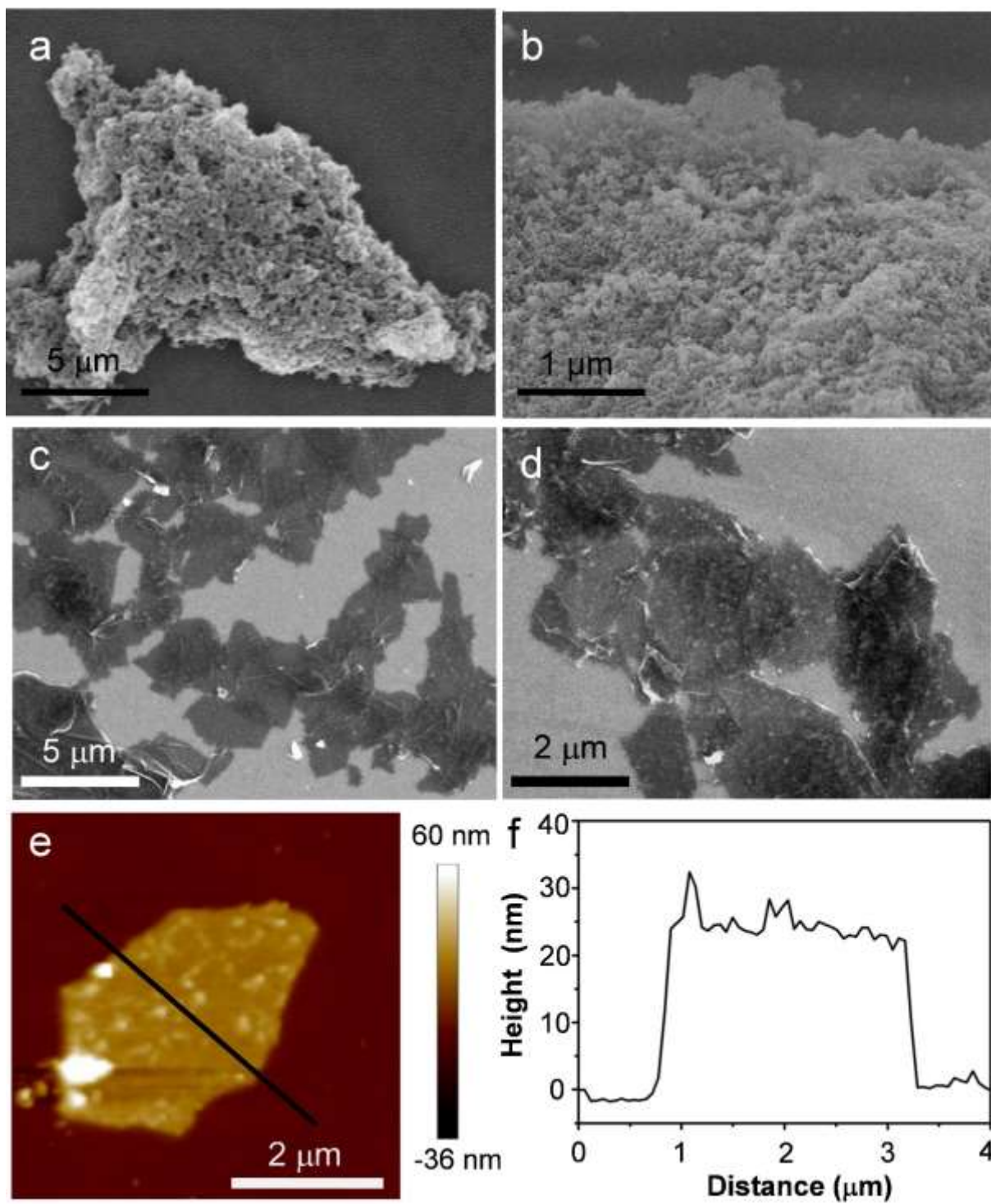


**Figure S4.** SEM images of pure CMPs (a, b) and CMPs/rGO (c, d), and AFM image (e) and the corresponding height profile (f) of CMPs/rGO nanosheets without ferrocene moieties

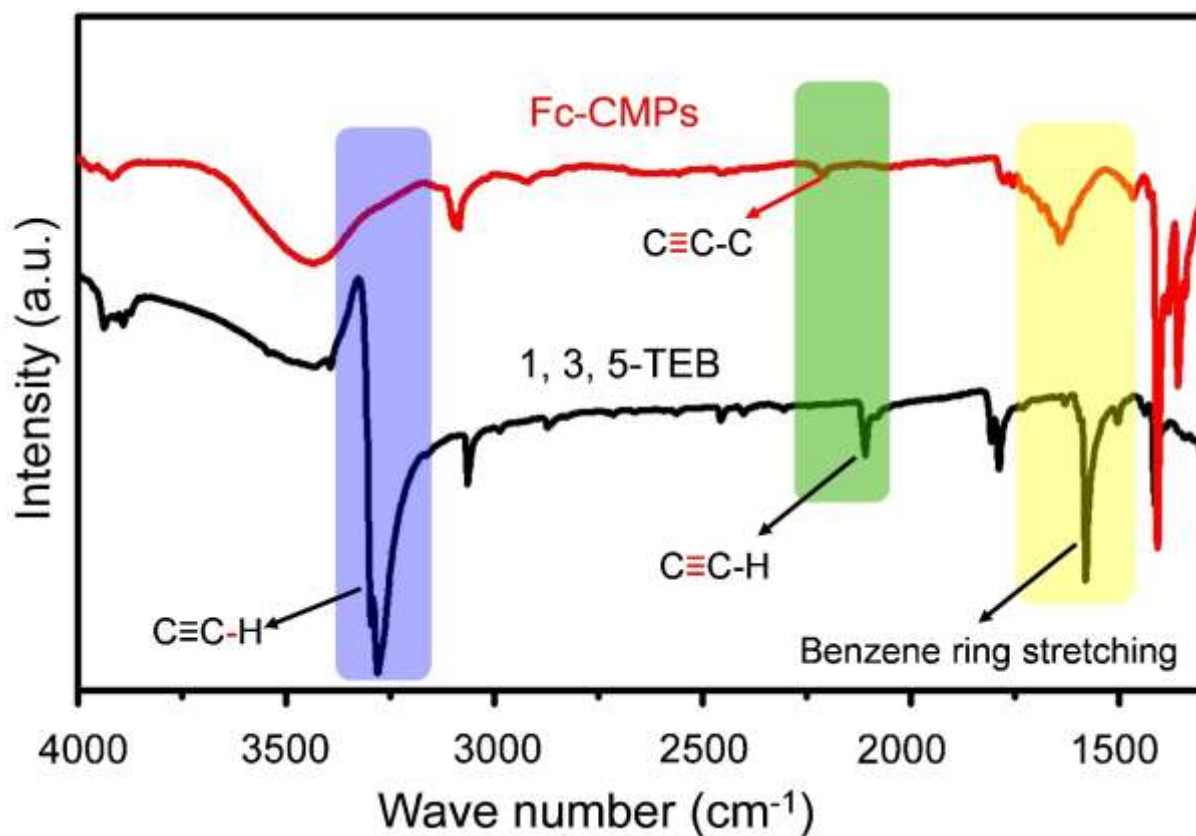


**Figure S5.** FT-IR spectra of 1, 3, 5-triethynylbenzene (1, 3, 5-TEB, black curve) and Fc-CMPs (red curve).

The polymerization process is monitored by FT-IR spectra. On one hand, the peak at  $2100\text{ cm}^{-1}$ , corresponding to the  $\text{C}\equiv\text{C}$  triple bond stretching of 1, 3, 5-TEB monomer, shifts to  $2200\text{ cm}^{-1}$  in Fc-GMP due to replacement of H with C after polymerization. On the other hand, C-H stretching at  $3300\text{ cm}^{-1}$  totally disappears, indicating the loss of H due to complete Sonogashira-Hagihara polymerization.

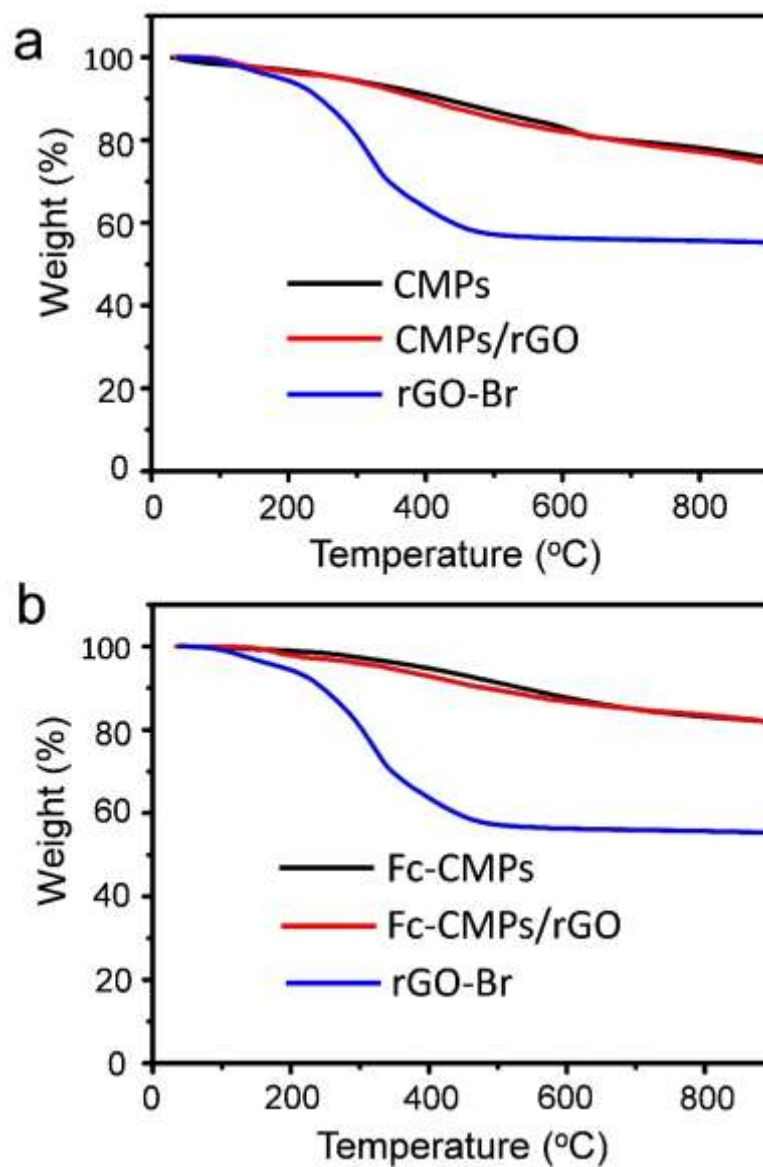


**Figure S6.** TGA analysis of rGO-Br, pure CMPs, CMPs/rGO, pure Fc-CMPs and Fc-CMPs/rGO.

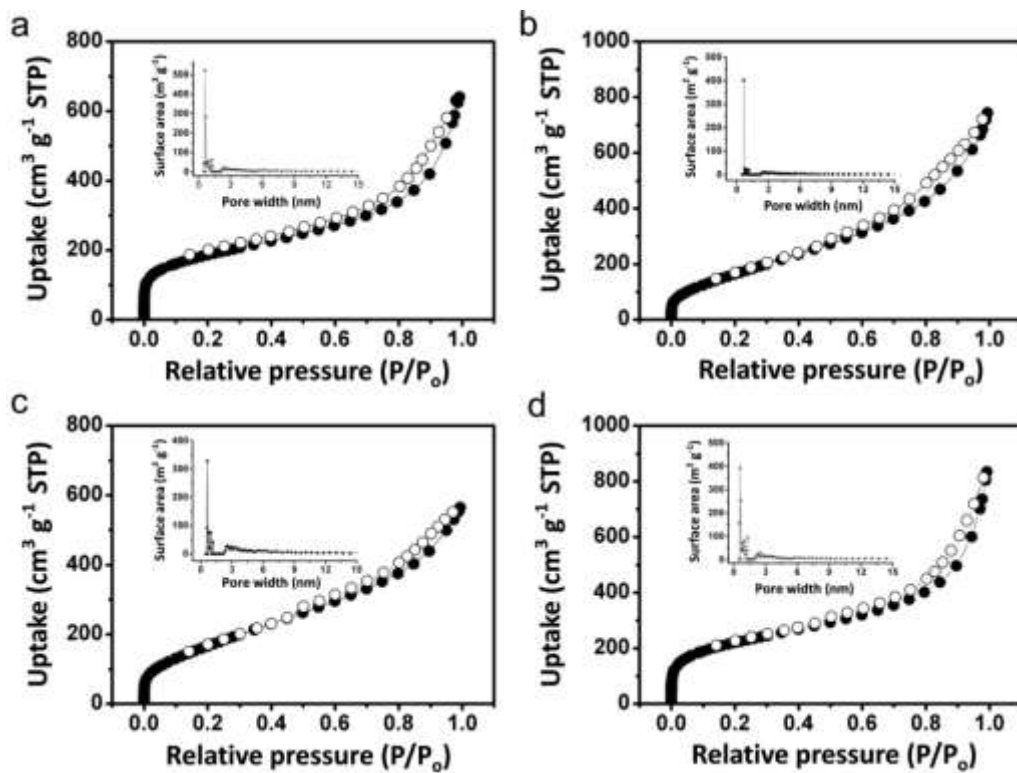


**Figure S7.**  $\text{N}_2$  sorption and pore size distribution of pure CMPs (a), CMPs/rGO (b), pure Fc-CMPs (c) and Fc-CMPs/rGO (d). The corresponding pore size distribution curves are given in the inset of each figure.

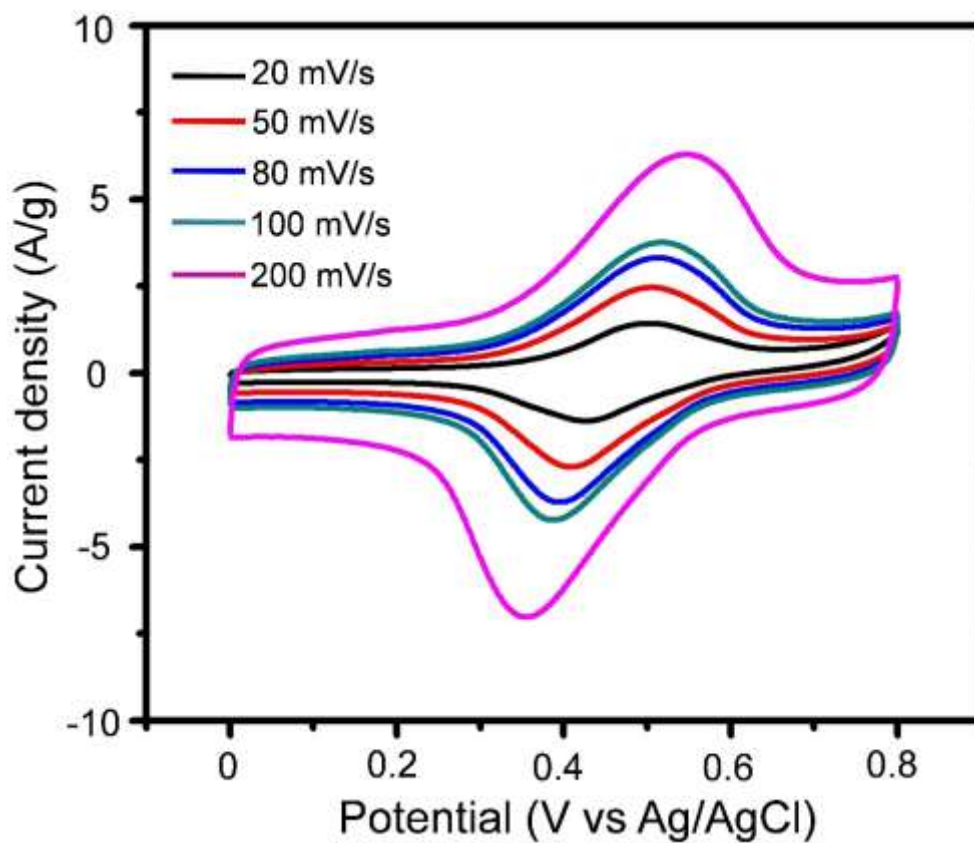


**Figure S8.** CV curves of Fc-CMPs at different scan rate in 1M H<sub>2</sub>SO<sub>4</sub>, clearly showing the redox peaks.

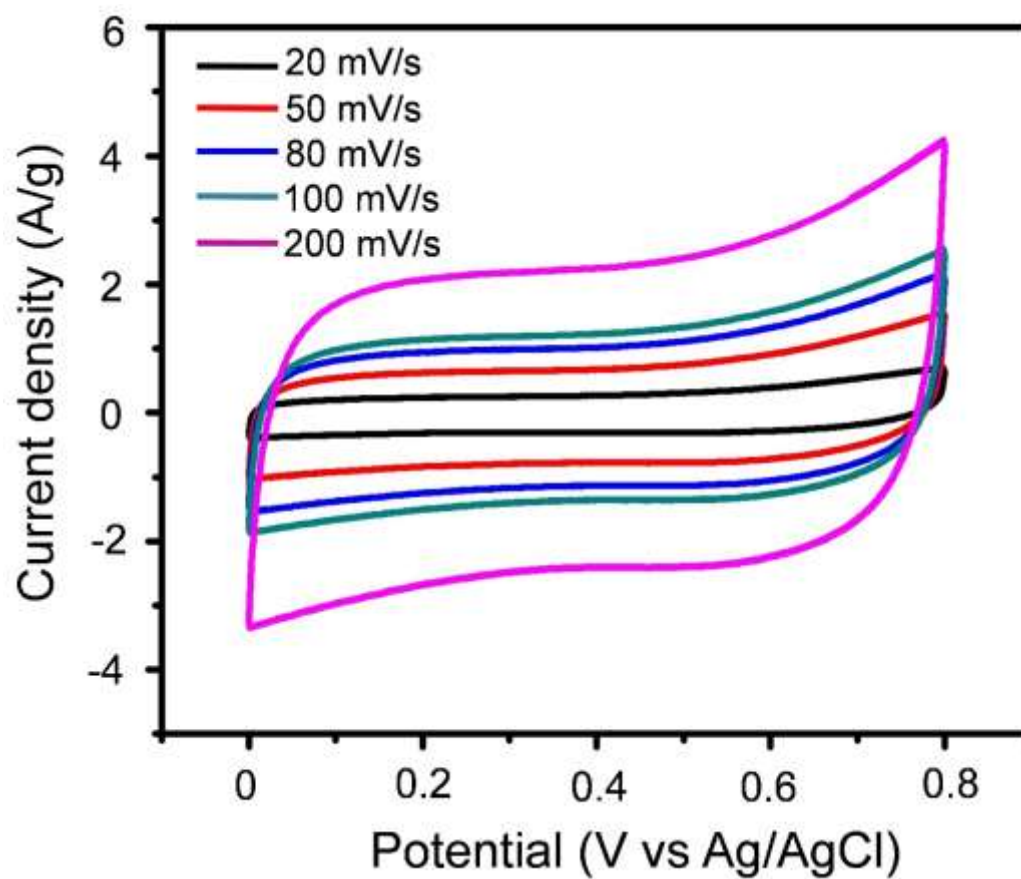


**Figure S9.** CV curves of pure CMPs at different scan rate in 1M H<sub>2</sub>SO<sub>4</sub>.

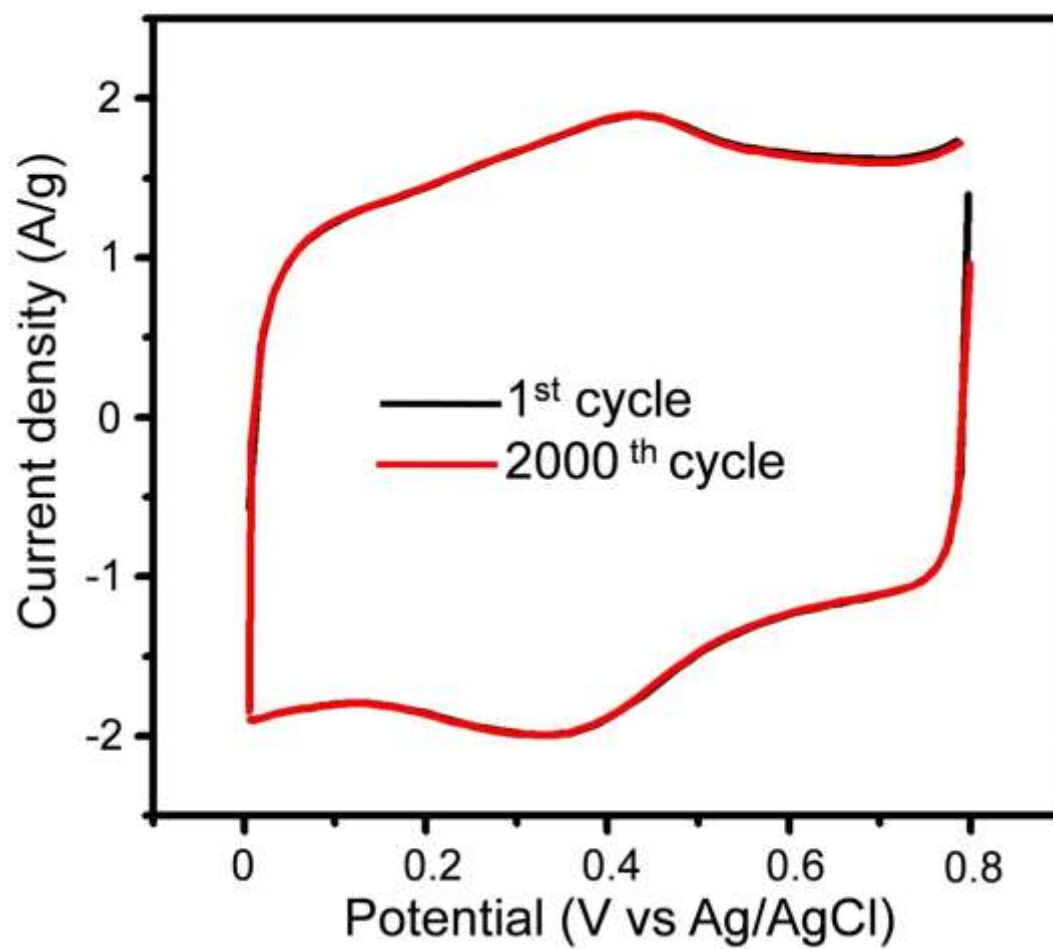


**Figure S10.** CV curves of Fc-CMPs/rGO on the 1<sup>st</sup> and 2000<sup>th</sup> cycles at 80 mV/s, showing good cycling stability.

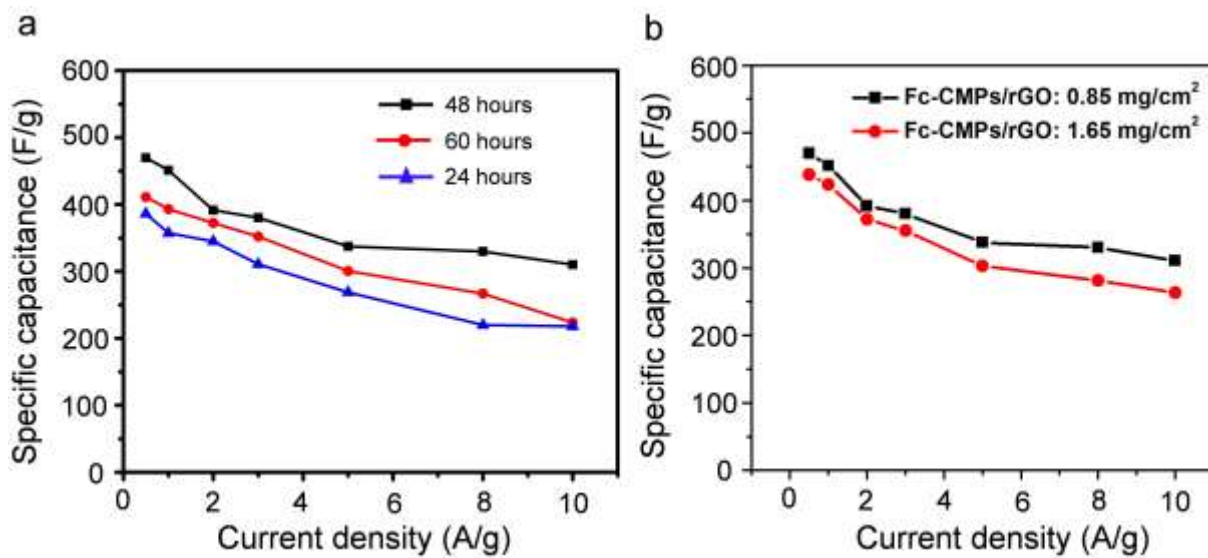


**Figure S11.** Specific capacitance of Fc-CMPs/rGO samples obtained with different polymerization time (a) and mass loading (b).

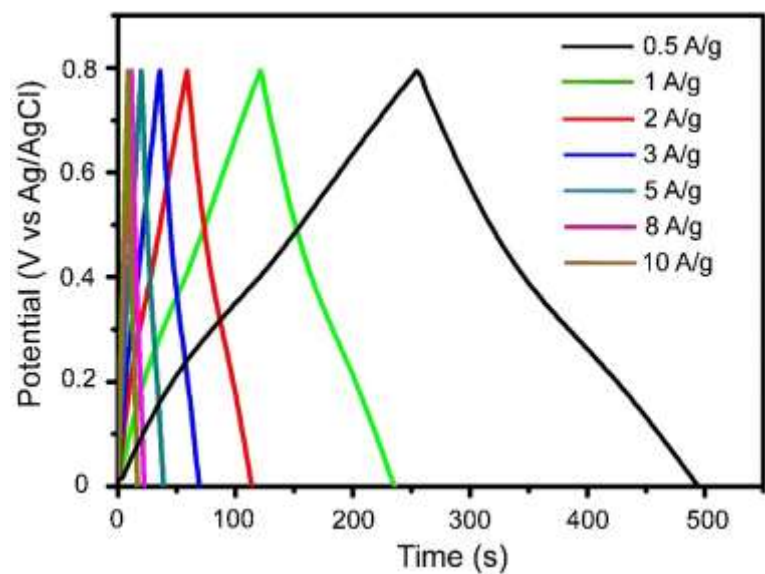


**Figure S12.** Charge-discharge curves of pure Fc-CMPs at current density of 0.5-10 A g<sup>-1</sup> in 1M H<sub>2</sub>SO<sub>4</sub>.

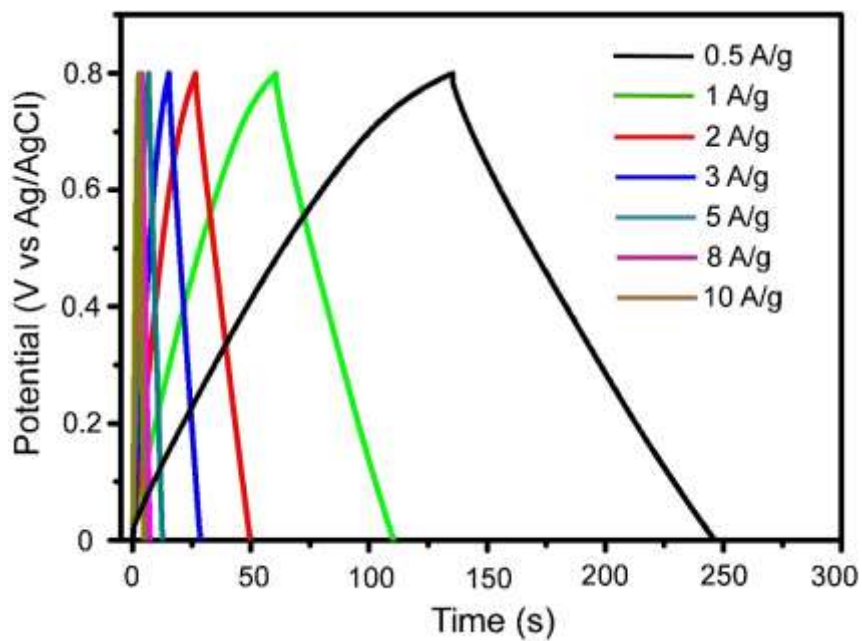


**Figure S13.** Charge-discharge curves of pure CMPs at current density of 0.5-10 A g<sup>-1</sup> in 1 M H<sub>2</sub>SO<sub>4</sub>.

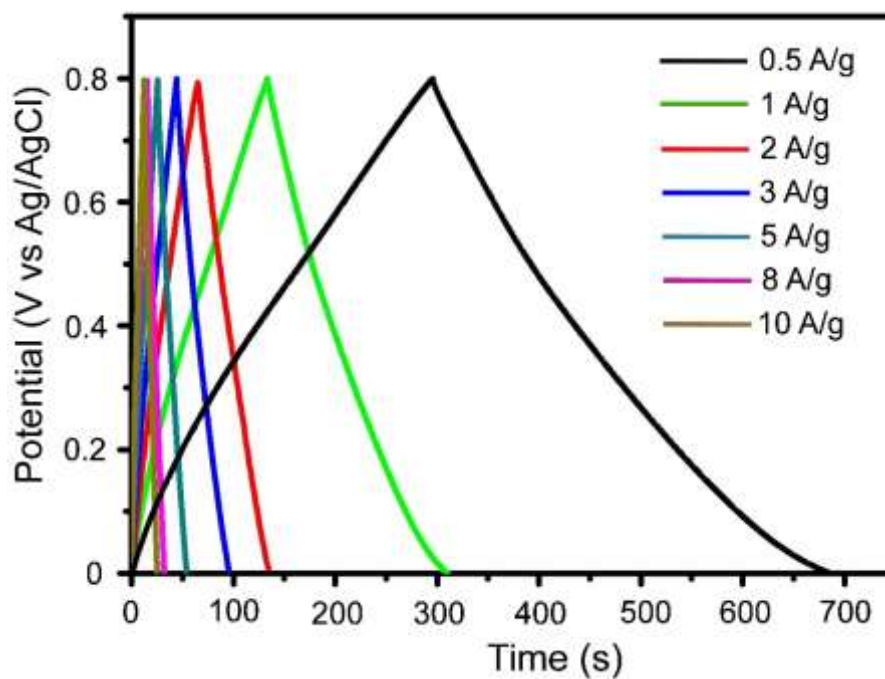


**Figure S14.** Charge-discharge curves of CMPs/rGO at current density of 0.5-10 A g<sup>-1</sup> in 1 M H<sub>2</sub>SO<sub>4</sub>.

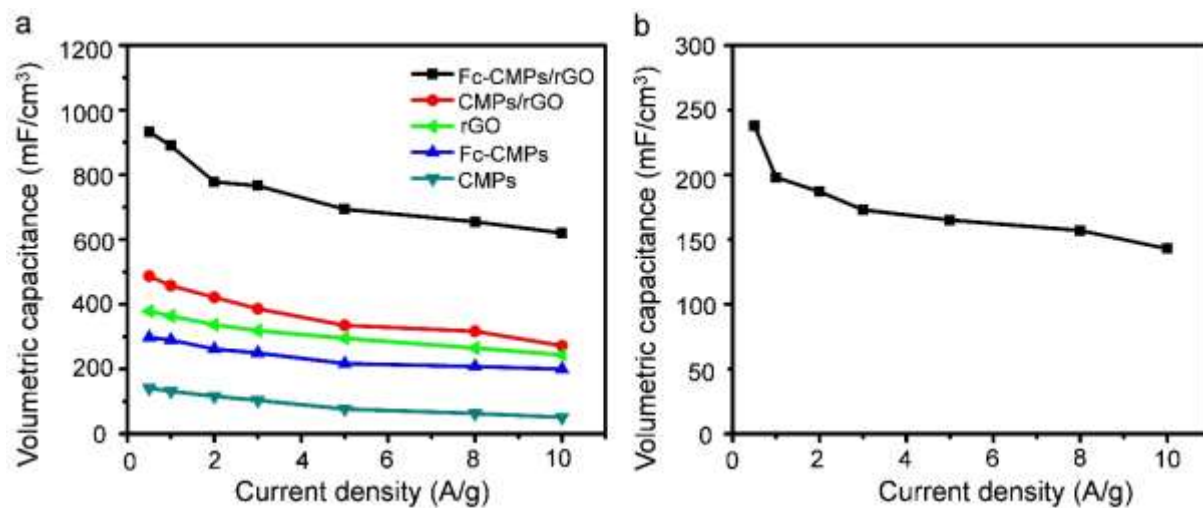


**Figure S15.** Volumetric capacitance of various electrodes in three-electrode system (a) and Fc-CMPs/rGO in two-electrode system (b).

**Table S1.** Structural properties of polymer networks calculated based on nitrogen adsorption analysis

	BET surface area (m <sup>2</sup> /g)	Pore size (nm)
CMPs	672.3	0.6, 0.7, 1.0
CMPs/rGO	668.3	0.6, 0.9, 1.1
Fc-CMPs	653.2	0.7, 0.9, 1.1
Fc-CMPs/rGO	800.1	0.6, 0.7, 1.3

**Table S2.** Summary of various electrochemical resistance values for pure CMPs, pure Fc-CMPs, CMPs/rGO and Fc-CMPs/rGO.

	CMPs	Fc-CMPs	CMPs/rGO	Fc-CMPs/rGO
R <sub>o</sub> (Ω)	9.03	7.12	6.82	6.59
R <sub>ct</sub> (Ω)	959.20	917.50	29.43	8.48

**Table S3.** Performance comparison of Fc-CMPs/rGO with the reported, highly-efficient, polymer and carbon materials-based supercapacitors.

Material	Specific capacitance (F g <sup>-1</sup> )	Current density	Electrode system	Cyclic performance (retention)	Ref.
<b>Fc-CMPs/rGO</b>	<b>231</b>	<b>0.5 A g<sup>-1</sup></b>	<b>2-electrode CD</b>	<b>95 % after 8000 cycles at 3A g<sup>-1</sup></b>	<b>This work</b>
<b>Fc-CMPs/rGO</b>	<b>470/310</b>	<b>0.5/10 A g<sup>-1</sup></b>	<b>3-electrode CD</b>		
Graphene/microporous polymer	244-304	0.1A g <sup>-1</sup>	3-electrode CD		3
graphene nanoribbons and carbon nanorods	187	50 mA g <sup>-1</sup>	2-electrode CD	75 % after 8000 cycles at 10 mV s <sup>-1</sup>	4
$\beta$ -Ketoenamine-Linked Covalent Organic Frameworks (COF)	48	0.1 A g <sup>-1</sup>	3-electrode CD	83.3 % after 5000 cycles at 0.1 A g <sup>-1</sup>	5
Graphene-Polyaniline paper	763/490	1/10 A g <sup>-1</sup>	3-electrode CD	82 % after 1000 cycles at 5 A g <sup>-1</sup>	6
Graphene/microporous polymer	304	0.1 A g <sup>-1</sup>	3-electrode CD	--	7
Graphene-CMP sandwiches	179	0.2 A g <sup>-1</sup>	3-electrode CD	--	7
Conductive metal organic framework (CMOF)	202	0.5 A g <sup>-1</sup>	3-electrode CD	80 % after 5000 cycles at 800 mV s <sup>-1</sup>	8
Pyridine-based COF	209	0.5 A g <sup>-1</sup>	3-electrode CD	92 % after 6000 cycles at 2 A g <sup>-1</sup>	9
Conductive MOF	111	0.05 A g <sup>-1</sup>	3-electrode CD	90 % after 10000 cycles at 2 A g <sup>-1</sup>	10
3D polyaminoanthraquinone	576	1 A g <sup>-1</sup>	3-electrode CD	80-85% after 6000 cycles	11
	168	2 A g <sup>-1</sup>	2-electrode CD	95.5% after 2000 cycles	
Tetracyanoquinodimethane-derived conductive microporous covalent triazine-based frameworks (TCNQ-CTFs) derived carbon	383	0.2 A g <sup>-1</sup>	3-electrode CD	No decay after 10000 cycles	12
Ni-Hexaaminobenzene MOF (Ni-HAB)	427	10 A g <sup>-1</sup>	3-electrode CD	90% after 12000 cycls	13

## References

1. A. M. Khattak, H. Yin, Z. A. Ghazi, B. Liang, A. Iqbal, N. A. Khan, Y. Gao, L. Li, Z. Tang, Three dimensional iron oxide/graphene aerogel hybrids as all-solid-state flexible supercapacitor electrodes. *RSC Adv.* **2016**, *6*, 58994.
2. K. Zhang, L. Mao, L. L. Zhang, H. S. On Chan, X. S. Zhao, J. Wu, Surfactant-intercalated, chemically reduced graphene oxide for high performance supercapacitor electrodes. *J. Mater. Chem.* **2011**, *21*, 7302.
3. X. Zhuang, F. Zhang, D. Wu, N. Forler, H. Liang, M. Wagner, D. Gehrig, M. R. Hansen, F. Laquai, X. Feng, Two-Dimensional Sandwich-Type, Graphene-Based Conjugated Microporous Polymers. *Angew. Chem. Int. Ed.* **2013**, *52*, 9668.
4. P. Pachfule, D. Shinde, M. Majumder, Q. Xu, Fabrication of carbon nanorods and graphene nanoribbons from a metal–organic framework. *Nature Chemistry* **2016**, *8*, 718.
5. C. R. DeBlase, K. E. Silberstein, T.-T. Truong, H. D. Abruña, W. R. Dichtel,  $\beta$ -Ketoenamine-Linked Covalent Organic Frameworks Capable of Pseudocapacitive Energy Storage. *J. Am. Chem. Soc.* **2013**, *135*, 16821.
6. H.-P. Cong, X.-C. Ren, P. Wang, S.-H. Yu, Flexible graphene-polyaniline composite paper for high-performance supercapacitor. *Energy Environ. Sci.* **2013**, *6*, 1185.
7. K. Yuan, G.- P. Wang, T. Hu, L. Shi, R. Zeng, M. Forster, T. Pichler, Y. Chen, U. Scherf, Nanofibrous and Graphene-Templated Conjugated Microporous Polymer Materials for Flexible Chemosensors and Supercapacitors. *Chem. Mater.* **2015**, *27*, 7403.
8. W.-H. Li, K. Ding, H.-R. Tian, M.-S. Yao, B. Nath, W.-H. Deng, Y. Wang, G. Xu, Conductive Metal–Organic Framework Nanowire Array Electrodes for High-Performance Solid-State Supercapacitors. *Adv. Funct. Mater.* 1702067-n/a.
9. A. M. Khattak, Z. A. Ghazi, B. Liang, N. A. Khan, A. Iqbal, L. Li, Z. Tang, A redox-active 2D covalent organic framework with pyridine moieties capable of faradaic energy storage. *J. Mater. Chem. A* **2016**, *4*, 16312.
10. D. Sheberla, J. C. Bachman, J. S. Elias, C.-J. Sun, Y. Shao-Horn, M. Dinca, Conductive MOF electrodes for stable supercapacitors with high areal capacitance. *Nat. Mater.* **2017**, *16*, 220.
11. Y. Liao, H. Wang, M. Zhu, A. Thomas, Efficient Supercapacitor Energy Storage Using Conjugated Microporous Polymer Networks Synthesized from Buchwald–Hartwig Coupling. *Adv. Mater.* **2018**, *30*, 1705710
12. Y. Li, S. Zheng, X. Liu, P. Li, L. Sun, R. Yang, S. Wang, Z.-S. Wu, X. Bao, W.-Q. Deng, Conductive Microporous Covalent Triazine-Based Framework for High-Performance

Electrochemical Capacitive Energy Storage. *Angew. Chem. Int. Ed.* **2018**, DOI: 10.1002/anie.201711169

13. D. Feng, T. Lei, M. R. Lukatskaya, J. Park, Z. Huang, M. Lee, L. Shaw, S. Chen, A. A. Yakovenko, A. Kulkarni, J. Xiao, K. Fredrickson, J. B. Tok, X. Zou, Y. Cui, Z. Bao, Robust and conductive two-dimensional metal–organic frameworks with exceptionally high volumetric and areal capacitance. *Nature Energy*, **2018**, 3, 30.